NUKLEONIKA 2017;62(2):109–115
doi: 10.1515/nuka-2017-0015

ORIGINAL PAPER

DE GRUYTER OPEN

© 2017 Robert Konieczny *et al*. This is an open access article distributed under the Creative Commons Attribution -NonCommercial-NoDerivatives 3.0 License (CC BY-NC-ND 3.0).

Thermodynamic properties of dilute Co-Fe solid solutions studied by ^{57}Fe Mössbauer spectroscopy

Robert Konieczny, Rafał Idczak

Abstract. The $Co_{1-x}Fe_x$ alloys where x ranges from 0.01 to 0.06 were measured at room temperature using transmission Mössbauer spectroscopy (TMS). The analysis of the obtained data allowed the determination of the short-range order (SRO), the binding energy E_b between two iron atoms in the studied materials using the extended Hrynkiewicz-Królas idea and the enthalpy of solution $H_{Co\text{-}Fe}$ of Fe in Co. The results showed that the Fe atoms dissolved in a Co matrix interact repulsively and the estimated value of $H_{Co\text{-}Fe} = -0.166(33)$ eV/atom. Finally, values of the enthalpy of solution were used to predict the enthalpy of mixing for the Co-Fe system. These findings were compared with corresponding data given in the literature, which were derived from calorimetric experiments and from the cellular atomic model of alloys described by Miedema.

Keywords: Mössbauer spectroscopy • binding energy • short-range order • enthalpy of solution • enthalpy of mixing • binary alloys

Introduction

The cobalt-iron alloys are promising for the development of new engineering materials. The systems are attracting much attention because of their unique combination of several important properties such as high saturation magnetization, high Curie temperature, low magnetocrystalline anisotropy and good strength. Moreover, the materials are characterized by a low susceptibility to surface fissures in the rolling process which is of special interest for metallurgy. It is worth noticing that significant amounts of research and developments over the years have been really fruitful and resulted, for example, in significant improvements in terms of mechanical properties and a more comprehensive understanding of phase transformations in Co-Fe alloys. As a result of all of the above Co-Fe alloys are attractive materials for many applications, even at elevated temperatures. In particular, these alloys are used in the production of turbine engine components, transformers, magnetic bearings and recording heads [1–5]. At the same time, this system is regarded as a model for experimental and theoretical studies of thermodynamic properties [6–8].

By taking into account the unique characteristics of the Co-Fe system mentioned above, ^{57}Fe Mössbauer spectroscopy was applied to the study of the $Co_{1-x}Fe_x$ series of solid solutions with low concentrations of iron in order to improve the knowledge about properties of this system, especially thermodynamic ones. Mössbauer spectroscopy delivers information on many characteristics of solids, in particular on the types of impurity interactions, the enthalpies of

R. Konieczny✉, R. Idczak
Institute of Experimental Physics,
University of Wroclaw,
9 M. Borna Sq., 50-204 Wrocław, Poland,
Tel.: +48 71 375 9336, Fax: +48 71 328 7365,
E-mail: robi@ifd.uni.wroc.pl

Received: 27 June 2016
Accepted: 30 September 2016

solution of elements in the ferromagnetic matrix as well as the short-range order (SRO) [9–15]. In some cases the information concerning the enthalpy of solution obtained this way is unique, i.e. impossible to obtain with, for example, commonly used calorimetric methods [16, 17]. Calorimetric methods performed at relatively high temperatures, usually above Curie temperatures, do not facilitate the observation of the influence of magnetic interactions on thermodynamic properties of the alloys studied, i.e. the Co-Fe series. Moreover, the Mössbauer enthalpy-of-solution data can be used to predict the enthalpy of mixing of the system under consideration as a result of the appropriate relationship given by Sluiter and Kawazoe [18]. To the best of our knowledge, Mössbauer spectroscopy has yet to be used for such predictions in the case of the Co-Fe system.

The aim of this work was to apply ^{57}Fe Mössbauer spectroscopy for the determination of hyperfine interactions and thermodynamic parameters of dilute Co-Fe solid solutions and then thermally annealed ones.

Experimental and results

Preparation of samples

The $Co_{1-x}Fe_x$ alloy samples where x ranges from 0.01 to 0.06 were prepared by arc melting. Appropriate amounts of the high-purity components (99.99% pure cobalt and 99.8% pure ^{57}Fe isotope) were melted in an argon atmosphere and quickly cooled to room temperature. The weight losses during the melting process were below 1% so the compositions of the obtained alloys were close to nominal ones. In the next step, the obtained ingots were cold-rolled to a final thickness of about 0.04 mm and then the resulting foils were annealed in a vacuum at 1270 K for 2 h. After the annealing process the samples were slowly cooled to room temperature over 6 h. As a result, the alloys were homogeneous and free from structural defects such as vacancies or dislocations. Finally, it is worth noting that under these conditions, atomic diffusion effectively ceases at a certain temperature T_d, so the distribution of atoms observed in the annealed specimens should be frozen-in state at this temperature.

Measurements

The TMS measurements were performed at room temperature using a constant-acceleration POLON spectrometer of standard design and a 50 mCi ^{57}Co-in-Rh standard source with a full width at half maximum (FWHM) of 0.22 mm/s. The ^{57}Fe Mössbauer spectra for each $Co_{1-x}Fe_x$ sample were recorded twice, before and after the annealing process. Moreover, to estimate the T_d value, the duplicated Mössbauer spectra were measured for the alloy $Co_{0.94}Fe_{0.06}$ which was quenched from different temperatures (350–700 K). The obtained spectra are presented in Figs. 1–3.

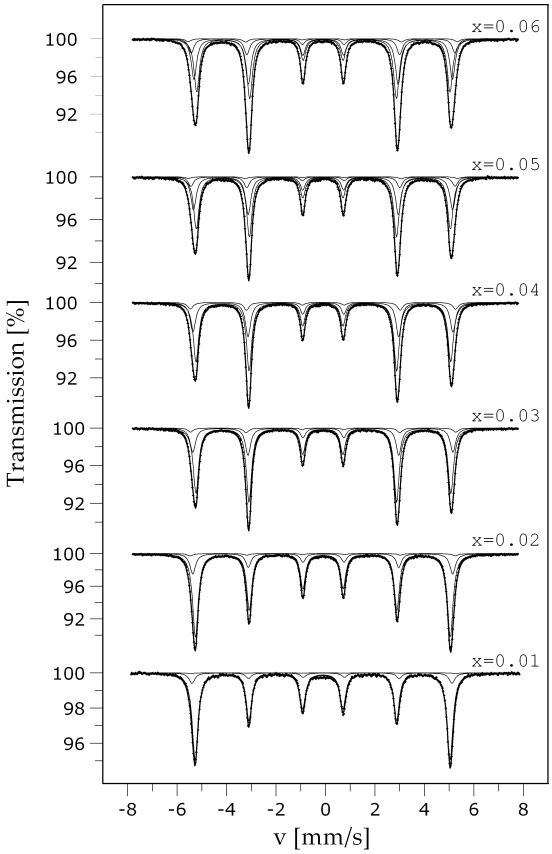

Fig. 1. Room-temperature ^{57}Fe Mössbauer spectra for the $Co_{1-x}Fe_x$ series of alloys measured just after being melted in an arc furnace.

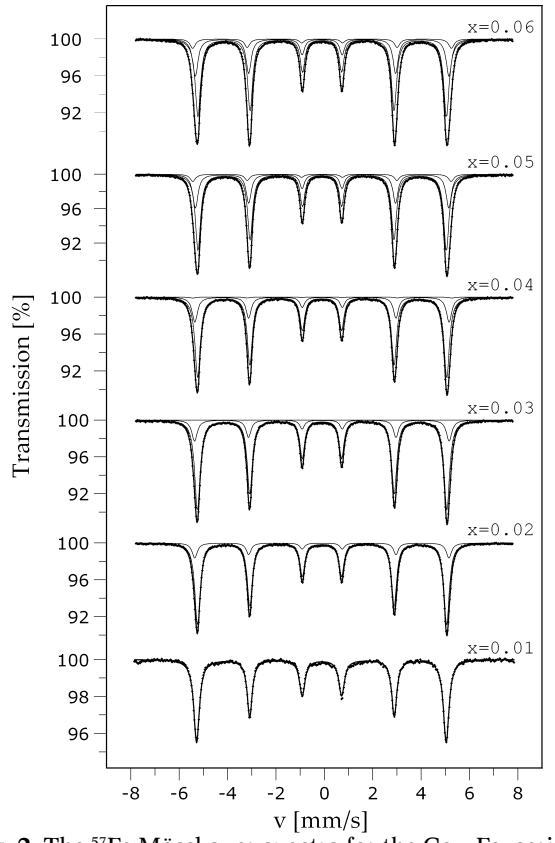

Fig. 2. The ^{57}Fe Mössbauer spectra for the $Co_{1-x}Fe_x$ series of alloys measured at room temperature after the annealing process at 1270 K and slowly being cooled to room temperature.

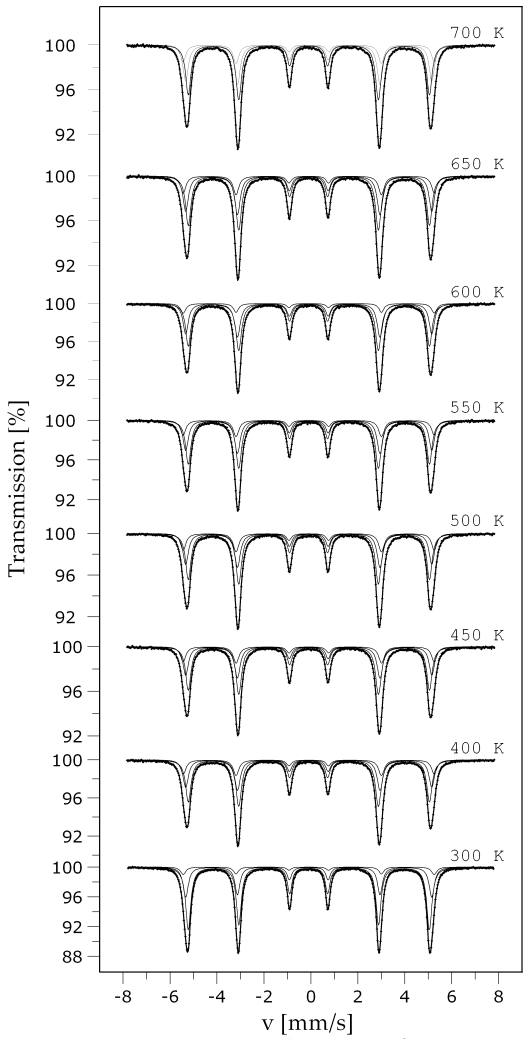

Fig. 3. Room-temperature ^{57}Fe Mössbauer spectra measured for samples of the $Co_{0.94}Fe_{0.06}$ alloy quenched from different temperatures.

Data analysis

The measured TMS spectra were fitted with a sum of different six-line components. These lines correspond to the various hyperfine fields B at ^{57}Fe nuclei generated by different numbers of Co and Fe atoms located in the first coordination shell of the nuclear probe. The number of fitted six-line spectral components depended on the concentration of Fe in the samples – three for all melting alloys before annealing but in the case of annealed samples it was one for $Co_{0.99}Fe_{0.01}$, two for $Co_{0.98}Fe_{0.02}$ and three for the others. The obtained fits are presented in Figs. 1 and 2. The fitting procedure for spectra with three components was conducted under the assumption (compare [9–13, 19]) that the influence of impurity atoms on the isomer shift IS as well as on the corresponding hyperfine field B of a subspectrum is additive and independent of the positions of atoms in the first coordination shell of the Mössbauer probe. Accordingly, it was assumed that for each subspectrum of the three-component spectra the quantities IS and B were linear functions of the number n of Fe atoms located in the first coordination shell of the ^{57}Fe nuclear probe. The functions could be expressed as follows:

$$\begin{aligned} \mathrm{IS}(n) &= \mathrm{IS}_0 + n\Delta\mathrm{IS} \\ B(n) &= B_0 + n\Delta B \end{aligned} \tag{1}$$

where ΔIS and ΔB stand for the changes in IS and B with one Fe atom in the first coordination shell of the nuclear probe. Finally, the quadrupole shift QS of a subspectrum was treated as a free parameter [20].

Generally, the assumptions presented above are sufficient to obtain sensible results. Unfortunately, as far as the investigated alloys are concerned, the presence of an Fe atom in the nearest coordination shell of ^{57}Fe generates small changes in IS and B, too small to perform a sufficient analysis of the Mössbauer spectra in terms of several components without additional assumptions. For successful analysis of these spectra it is necessary to use a second series of data. The first one for the samples just after the melting process, in which the atoms were in a frozen-in high temperature state and the second one for the samples after annealing at 1270 K for 2 h. The samples following the melting process can be treated as disorder alloys. In this case the probability of the existence of n iron atoms among all N atoms located in the first coordination shell of the ^{57}Fe could be described by the binomial distribution $p(n) = [N!/((N-n)!n!)]x^n(1-x)^{N-n}$. It is accepted that $N = 12$ for both high-temperature fcc and low-temperature hcp structures of the studied Co-Fe alloys [21]. The values of the parameters of the best-fit model which were obtained for the spectra are presented in Table 1. These values are in good agreement with corresponding data given in the literature [22, 23]. These values were used during the spectral analysis of the annealed samples.

As the main result of the analysis the values of relative contributions c_0, c_1 and c_2 of spectral components for the annealed samples were determined. Assuming that the Lamb-Mössbauer factor is independent of the

Table 1. Parameters of the hyperfine field and isomer shift obtained for Co-Fe alloys. The standard uncertainties for the parameters resulted from the variance of the fit. Values of the isomer shift IS_0 are reported relative to the corresponding value for α-Fe at room temperature

x	B_0 [T]	ΔB [T]	IS_0 [mm/s]	ΔIS [mm/s]
0.01	31.959(45)	–	–0.001(1)	–
0.02	31.918(37)	0.635(22)	0.013(6)	–0.001(1)
0.03	31.937(48)	0.655(18)	0.015(4)	–0.001(1)
0.04	31.905(44)	0.657(12)	0.016(4)	–0.001(1)
0.05	31.816(46)	0.639(12)	0.018(5)	–0.002(1)
0.06	31.837(57)	0.654(10)	0.018(3)	–0.001(1)

Table 2. The binding energy E_b between a pair of Fe atoms in the $Co_{1-x}Fe_x$ series of alloys deduced from the ^{57}Fe Mössbauer spectra. The standard uncertainties for c_0, c_1 and c_2 resulted from the variance of the fit of the assumed model to the spectra measured

x	c_0	c_1	c_2	p_0	p_1	E_b [eV]
0.01	1	–	–	0.8864	0.1074	–
0.02	0.8656(27)	0.1344(27)	–	0.7847	0.1922	0.02517(56)
0.03	0.8083(63)	0.1901(54)	0.0046(17)	0.6938	0.2575	0.02697(62)
0.04	0.7552(57)	0.2349(50)	0.0133(19)	0.6127	0.3064	0.02948(66)
0.05	0.6495(42)	0.2889(40)	0.0716(24)	0.5404	0.3413	0.02288(51)
0.06	0.5949(41)	0.3296(40)	0.1655(32)	0.4759	0.3645	0.02186(49)

configuration of atoms in the surroundings of the ^{57}Fe nucleus, the parameters c_0, c_1 and c_2 are intensities of the components of a spectrum which are related to the existence of 0, 1 and 2 iron atoms in the first coordination shell of nuclear probes of ^{57}Fe, respectively. The results are presented in Table 2.

The freezing temperature T_d for atoms in the dilute Co-Fe alloys

The freezing temperature T_d could be defined as a temperature below which atomic diffusion in the material practically does not exist. The temperature T_d for the dilute binary iron alloys could be determined from the temperature studies performed for instance by ^{57}Fe Mössbauer spectroscopy. In this work, to estimate the value of T_d for Co-Fe alloys of low iron content, the duplicate Mössbauer spectra were measured for the alloy $Co_{0.94}Fe_{0.06}$ which was quenched from different temperatures (350–700 K). These spectra, which are presented in Fig. 3, were analysed as above in terms of the c_1 and c_2 parameters, which characterize the atomic surroundings of the nuclear probes. The results are listed in Fig. 4. As can be seen, the value of each parameter practically does not change as the temperature increases up to about 500 K. This indicates a lack of atomic diffusion in the alloy. Whereas at higher temperatures there is significant temperature dependence of the parameters mentioned. It follows that at these temperatures

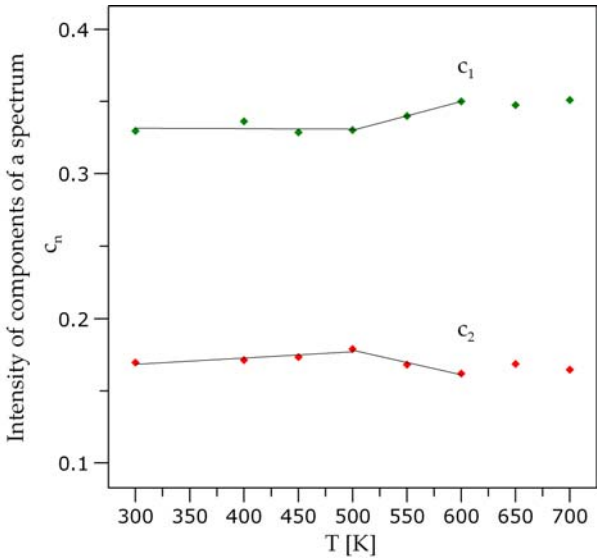

Fig. 4. Temperature dependence of the c_1 and c_2 parameters for the $Co_{0.94}Fe_{0.06}$ alloy.

the diffusion of atoms in the alloy is possible. The temperature dependences of the c_1 and c_2 parameters were used for the estimation of the freezing temperature T_d in the $Co_{0.94}Fe_{0.06}$ alloy assuming that both dependences $c_1(T)$ and $c_2(T)$ can be approximated by two straight lines, which intersect when $T = T_d$. The parameters of the lines were found by fitting them separately to the c_1 and c_2 values at temperatures T within two ranges 300 K ≤ T ≤ 500 K and 500 K ≤ T ≤ 700 K. The T_d determined in this way was equal to 500(11) K. Moreover, one can see in Fig. 4 that the obtained values of c_1 and c_2 at temperatures $T \geq 650$ K show further changes as temperature increases. This behaviour can be caused by the change in crystalline structure of the Co-Fe alloy from hcp to fcc, which occurs at about 700 K [24].

The binding energy E_b of two Fe atoms in the Co matrix

The calculation of the binding energy E_b for pairs of Fe atoms were based on the modified Hrynkiewicz-Królas formula [25], where E_b is presented as follows:

$$E_b = -kT_d \ln\left((1 + 2c_1/c_0)\cdot(c_1/c_0)\cdot(1 + 2\,p_1/p_0)^{-1}\cdot(p_1/p_0)^{-1}\right) \quad (2)$$

This formula uses the values of the relative contributions c_0 and c_1 of spectral components of annealed samples. In the above equation k is the Boltzmann constant, whereas T_d is the "freezing" temperature for the atomic distribution in an annealed sample of $Co_{1-x}Fe_x$ and in this case it amounted to T_d = 500(11) K whereas p_0 and p_1 are probabilities of the existence of 0 and 1 iron atoms among all N atoms located in the first coordination shell of the ^{57}Fe nuclear probe, given by the binomial distribution for the hcp lattice where N = 12. Computed E_b values are presented in Table 2.

The extrapolated value of the binding energy E_b (x = 0) was calculated using the E_b values derived from data obtained for samples with the smallest iron content. Such a choice of E_b values was determined by the fact that the Hrynkiewicz-Królas model of E_b was proposed for alloys with a very low concentration of impurity atoms. The $E_b(0)$ was calculated to be 0.0276(55) eV. The positive values of the binding energies for all annealed samples indicate that iron atoms dissolved in the Co matrix interact repulsively.

Table 3. An enthalpy $H_{\text{Co-Fe}}$ [eV/atom] of solution of iron in cobalt

Calorimetric data [16]	Miedema's model [27]	This work
–0.120	–0.024	–0.166(33)

The enthalpy of solution of iron in cobalt

An extrapolated value of $E_b(0)$ was used to obtain an enthalpy of solution $H_{\text{Co-Fe}}$ of Fe in Co. By using the Hrynkiewicz-Królas model for the binding energy the calculations were conducted in the following way [26]:

$$H_{\text{Co-Fe}} = -z \cdot E_b(0)/2 \tag{3}$$

where z is the coordination number of the crystalline lattice ($z = 12$ for the hcp lattice of cobalt). The value of $H_{\text{Co-Fe}}$ is listed in Table 3 with corresponding enthalpies of solution obtained by calorimetric experiments [16],

$$H_{\text{Co-Fe}} = [\mathrm{d}H^{for}/\mathrm{d}x]_{x=0} \tag{4}$$

and calculated using Miedema's model of binary alloys [27].

A short-range order parameter

In the dilute $Co_{1-x}Fe_x$ systems the distribution of impurity atoms of iron is in most cases different from the binomial distribution. The short-range order parameter (SRO) α quantitatively describes deviation mentioned above as follows [28]:

$$\alpha = \frac{\langle n \rangle - x}{1 - x} \tag{5}$$

where $<n>$ is the average number of iron atoms in a given surroundings of an Fe atom.

The parameter α can be easily determined for the studied alloys from the Mössbauer spectra using the parameter c_n because it is related to the number $<n>$. When the number concerns the first coordination shell of the nuclear probe, the proper relationship is as follows:

$$\langle n \rangle = \frac{1}{12} \sum n c_n \tag{6}$$

The values of SRO parameters α for $Co_{1-x}Fe_x$ alloys are presented in Table 4 and Fig. 5. Negative values of α for all studied samples indicate that among the nearest neighbours of the ^{57}Fe nuclear probe, there are far less iron atoms than expected for a random case. This means that, the interaction between two iron atoms is repulsive, i.e. the Co-Fe bonds are predominant. This fact confirms our findings presented in the section concerning the binding energy of two iron atoms in the cobalt matrix.

Table 4. The SRO parameters α for the $Co_{1-x}Fe_x$ series of alloys deduced from the ^{57}Fe Mössbauer spectra

x	α
0.02	–0.00898(23)
0.03	–0.01432(87)
0.04	–0.01956(82)
0.05	–0.01648(65)
0.06	–0.01945(65)

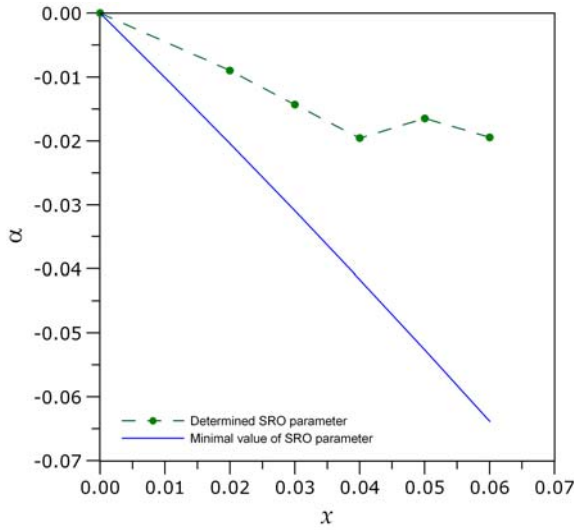

Fig. 5. The short-range order parameter α as a function of the concentration x of Fe atoms in the $Co_{1-x}Fe_x$ series of alloys. The minimum value of the SRO parameter is described by $\alpha = -x/(1-x)$.

The enthalpy of mixing curve for the Co-Fe solid solutions

The obtained $H_{\text{Co-Fe}}$ value could be used to determine the enthalpy of mixing H_{mix} for the Co-Fe alloys as follows [18]:

$$H_{\text{mix}}(x) \approx H_{\text{Co-Fe}}\, x^2(1-x) + H_{\text{Fe-Co}}\, x(1-x)^2 \tag{7}$$

where $H_{\text{Fe-Co}}$ is the enthalpy of solution of cobalt in iron. On the basis of Eq. (7) the $H_{\text{mix}}(x)$ dependence was calculated using the $H_{\text{Fe-Co}}$ value obtained previously [29]. The findings are presented in Fig. 6 together with the results of calculations using CALPHAD [6]; the corresponding values obtained

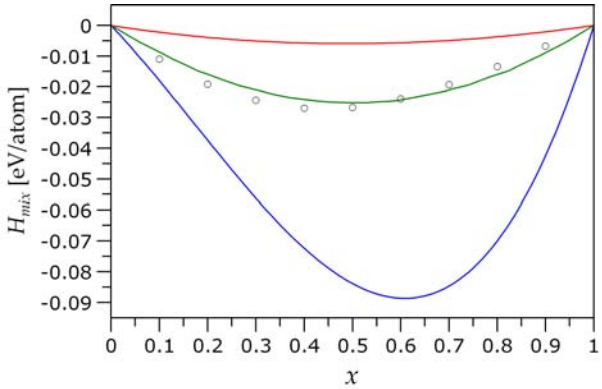

Fig. 6. Enthalpy of mixing H_{mix} for the $Co_{1-x}Fe_x$ series of alloys obtained in this work (blue line); computed by a CALPHAD calculation (green line); resulting from Miedema's model (red line); and derived from calorimetric measurements (circles).

from calorimetric measurements [7]; and the values resulting from Miedema's model [27].

Conclusions

The determined values of binding energies in the annealed $Co_{1-x}Fe_x$ alloys where x ranges from 0.01 to 0.06 are positive. These results indicate that the two iron atoms dissolved in the Co matrix interact repulsively. Moreover, the negative values of short-range order parameters α suggest the existence of ordering tendencies in the studied Co-Fe alloys, i.e. the predominance of Co-Fe bonds. This fact confirms our findings concerning the positive binding energies which were obtained using the Hrynkiewicz-Królas method.

An enthalpy of solution $H_{\text{Co-Fe}}$ of iron in cobalt obtained by ^{57}Fe Mössbauer spectroscopy is negative and equal to –0.166(33) eV/atom. This result is consistent with the corresponding value –0.120 eV/atom calculated from the heat of formation H^{for} of the Co-Fe systems derived from the calorimetric method. However, it is only in qualitative agreement with the value –0.024 eV/atom resulting from Miedema's model of alloys. This discrepancy could be explained by the fact that Miedema's model is based on measurements performed at high temperatures at which Co-Fe alloys are in a paramagnetic state.

The enthalpy of mixing of the Co-Fe system was determined for the first time using the Mössbauer spectroscopy technique. To estimate this important thermodynamic parameter, the relationship determined by Sluiter and Kawazoe [18] was used together with the enthalpy of solution of Fe in Co obtained in this work and previously estimated enthalpy of solutions of Co in Fe.

Acknowledgment. This work was supported by the University of Wrocław under the framework of project 0420/2010/IFD/16.

References

1. Sourmail, T. (2005). Near equiatomic FeCo alloys: constitution, mechanical and magnetic properties. *Prog. Mater. Sci.*, *50*, 816–880. DOI: 10.1016/j.pmatsci.2005.04.001.
2. Yu, R. H., Basu, S., Ren, L., Zhang, Y., Parvizi-Majidi, A., Unruh, K. M., & Xiao, J. Q. (2000). High temperature soft magnetic materials: FeCo alloys and composites. *IEEE Trans. Magn.*, *36*, 3388–3393. DOI: 10.1109/20.908809.
3. Fish, G. E. (1990). Soft magnetic materials. *Proc. IEEE 78*, 947–972. DOI: 10.1109/5.56909.
4. Fingers, R. T., & Rubertus, C. S. (2000). Application of high temperature magnetic materials. *IEEE Trans. Magn.*, *36*, 3373–3375. DOI: 10.1109/20.908805.
5. Sundar, R. S., & Deevi, S. C. (2005). Soft magnetic FeCo alloys: alloy development, processing, and properties. *Int. Mater. Rev.*, *50*, 157–192. DOI: 10.1179/174328005X14339.
6. Turchanin, M. A., Dreval, L. A., Abdulov, A. R., & Agraval, P. G. (2011). Mixing enthalpies of liquid alloys and thermodynamic assessment of the Cu–Fe–Co system. *Powder Metall. Met. Ceram.*, *50*, 98–116. DOI: 10.1007/s11106-011-9307-z.
7. Ohnuma, I., Enoki, H., Ikeda, O., Kainuma, R., Ohtani, H., Sundman, B., & Ishida, K. (2002). Phase equilibria in the Fe–Co binary system. *Acta Mater.*, *50*, 379–393. DOI: 10.1016/S1359-6454(01)00337-8.
8. Rodriguez, J. E., & Matson, D. M. (2015). Thermodynamic modeling of the solidification path of levitated Fe–Co alloys. *Calphad-Comput. Coupling Ph. Diagrams Thermochem.*, *49*, 87–100. DOI: http://dx.doi.org/10.1016/j.calphad.2015.03.001.
9. Konieczny, R., Idczak, R., & Chojcan, J. (2015). Interactions between osmium atoms dissolved in iron observed by the ^{57}Fe Mössbauer spectroscopy. *Nukleonika*, *60*(1), 75–79. DOI: 10.1515/nuka-2015-0016.
10. Konieczny, R., Idczak, R., & Chojcan, J. (2013). Mössbauer studies of interactions between titanium atoms dissolved in iron. *Hyperfine Interact.*, *219*, 121–127. DOI: 10.1007/s10751-012-0653-0.
11. Idczak, R., Konieczny, R., & Chojcan, J. (2013). Short-range order in iron alloys studied by ^{57}Fe Mössbauer spectroscopy. *Solid State Commun., 159*, 22–25. DOI: 10.1016/j.ssc.2013.01.015.
12. Chojcan, J. (2004). A dilute-limit heat of solution of 3d transition metals in iron studied with ^{57}Fe Mössbauer spectroscopy. *Hyperfine Interact.*, *156/157*, 523–529. DOI: 10.1007/978-1-4020-2852-6_76.
13. Konieczny, R., Idczak, R., Elsner, J., & Chojcan, J. (2012). An enthalpy of solution of platinum in iron studied by ^{57}Fe Mössbauer spectroscopy. *Hyperfine Interact.*, *206*, 119–124. DOI: 10.1007/s10751-011-0480-8.
14. Idczak, R., Konieczny, R., & Chojcan, J. (2013). Thermodynamic properties of Au-Fe alloys studied with ^{57}Fe Mössbauer spectroscopy. *Nukleonika*, *58*(1), 93–97.
15. Idczak, R., Konieczny, R., & Chojcan, J. (2012). Study of defects in Fe-Re and Fe-Mo alloys by the Mössbauer and positron annihilation spectroscopies. *Solid State Commun.*, *152*, 1924–1928. DOI: 10.1016/j.ssc.2012.07.027.
16. Hultgren, R., Desai, P. D., Hawkins, D. T., Gleiser, M., & Kelley, K. K. (1973). *Selected values of thermodynamic properties of binary alloys*. Metals Park, Ohio: American Society for Metals.
17. Swartzendruber, L. J., Itkin, V. P., & Alcock, C. B. (1993). *Phase diagrams of binary iron alloys*. Materials Park, Ohio: Materials Information Society.
18. Sluiter, M. H. F., & Kawazoe, Y. (2002). Prediction of the mixing enthalpy of alloys. *Europhys. Lett.*, *57*, 526–532. DOI: http://dx.doi.org/10.1209/epl/i2002-00493-3.
19. Vincze, I., & Campbell, I. A. (1973). Mössbauer measurements in iron base alloys with transition metals. *J. Phys. F-Metal Phys.*, *3*, 647–663. DOI: http://dx.doi.org/10.1088/0305-4608/3/3/023.
20. Falepin, A., Cottenier, S., Comrie, C. M., & Vantomme, A. (2006). Interpreting Mössbauer spectra reflecting an infinite number of sites: An application to $Fe_{1-x}Si$ synthesized by pulsed laser annealing. *Phys. Rev. B*, *74*, 184108. DOI: 10.1103/PhysRevB.74.184108.
21. Watanabe, D., Sekiguchi, T., Tanaka, T., Takahashi, M., Wakiyama, T., & Takahashi, M. (1983). Magnetic domains in hcp and dhcp Co-Fe alloys studied by 1 MV Lorentz electron microscopy. *J. Magn. Magn. Mater.*, *31/34*, 973–975. DOI: 10.1016/0304-8853(83)90759-X.

22. Johnson, C. E., Ridout, M. S., Cranshaw, T. E., & Madsen, P. E. (1961). Hyperfine field and atomic moment of iron in ferromagnetic alloys. *Phys. Rev. Lett*., *6*, 450–451. DOI: 10.1103/PhysRevLett.6.450.
23. Rao, G. N. (1985). Table of hyperfine fields for impurities in Fe, Co, Ni, Gd and Cr. *Hyperfine Interact*., *24/26*, 1119–1194. DOI: 10.1007/BF02354655.
24. Rodriguez, J. E., & Matson, D. M. (2015). Thermodynamic modeling of the solidification path of levitated Fe-Co alloys. *Calphad-Comput. Coupling Ph. Diagrams Thermochem.*, *49*, 87–100. DOI: 10.1016/j.calphad.2015.03.001.
25. Chojcan, J. (1998). Interaction between impurity atoms of 3d transition metals dissolved in iron. *J. Alloy. Compd.*, *264*, 50–53. DOI: 10.1016/S0925-8388(97)00264-8.
26. Królas, K. (1981). Correlation between impurity binding energies and heat of formation of alloys. *Phys. Lett. A*, *85*, 107–110. DOI: 10.1016/0375-9601(81)90235-8.
27. Miedema, A. R. (1992). Energy effects and charge transfer in metal physics, modeling in real space. *Physica B*, *182*, 1–17. DOI: 10.1016/0921-4526(92)90565-A.
28. Cowley, J. M. (1960). Short- and long-range order parameters in disordered solid solutions. *Phys. Rev*., *120*, 1648–1657. DOI: 10.1103/PhysRev.120.1648.
29. Idczak, R., Konieczny, R., Konieczna, Ż., & Chojcan, J. (2011). An enthalpy of solution of cobalt and nickel in iron studied with ^{57}Fe Mössbauer spectroscopy. *Acta Phys. Pol. A*, *119*, 37–40. DOI: 10.12693/APhysPolA.119.37.